ISSN 2413-5577, Ecological Safety of Coastal and Shelf Zones of Sea, 2024, No. 3, pp. 16–35.

Original article

Multiscale Eddies Dynamics in the Pacific Ocean Adjacent to the Kamchatka Peninsula and the Northern Kuril Islands

A. V. Zimin [1] *, **D. A. Romanenkov** [1], **A. A. Konik** [1], **O. A. Atadzhanova** [1, 2], **E. I. Svergun** [1], **A. I. Varkentin** [1, 3], **O. B. Tepnin** [1, 3]

[1] *Shirshov Institute of Oceanology of RAS, Moscow, Russia*

[2] *Marine Hydrophysical Institute of RAS, Sevastopol, Russia*

[3] *Kamchatka Branch of VNIRO, Petropavlovsk-Kamchatsky, Russia*

* *e-mail: zimin2@mail.ru*

Abstract

The Pacific Ocean shelf and continental slope off the Kamchatka Peninsula and the Northern Kuril Islands are the area of spawning and early stages of life for some commercial fish species. However, it remains a poorly studied area with a limited set of observational data. In this paper, we perform a comprehensive analysis of heterogeneous satellite observations and global tidal model results over March–August 2015–2021. The work aims to obtain new information on the spatial and temporal variability of the characteristics of different-scale eddy structures and to assess the influence of tidal dynamics on some features of this variability. The following open data archives and atlases are used: Mesoscale Eddy Trajectory Atlas Product Meta3.2 DT, Terra, Aqua/MODIS and VIIRS/Suomi NPP (ocean surface temperature, chlorophyll a), Sentinel-1A/B radar images, NASA SMAP wind, AVISO absolute dynamic topography, TPXO9 tidal currents, CMEMS GLORYS12v1 currents. The paper uses the analysis results to assess the interannual and seasonal variability of the incidence and characteristics of mesoscale and submesoscale eddies and its relation to variations in the East Kamchatka Current and wind regime. The contribution of the tide to the eddy dynamics is shown. As an example, we consider the case of manifestation of small eddies at the periphery of the mesoscale anticyclonic eddy in Avacha Bay. It is shown that the interaction of this anticyclonic structure with tidal currents can serve as an independent mechanism of submesoscale eddy generation. This finding can be extended to the entire study region, which appears to be important for understanding the factors affecting the survival of commercial fishes at early life stages.

Keywords: eddy, altimetry, radar, optical range, mesoscale eddies, submesoscale eddies, tide, currents, vorticity, pollock, Pacific Ocean

Acknowledgements: This work has been supported by the grants of the Russian Science Foundation № 23-17-00174, https://rscf.ru/project/23-17-00174/

For citation: Zimin, A.V., Romanenkov, D.A., Konik, A.A., Atadzhanova, O.A., Svergun, E.I., Varkentin, A.I. and Tepnin, O.B., 2024. Multiscale Eddies Dynamics in the Pacific Ocean Adjacent to the Kamchatka Peninsula and the Northern Kuril Islands. *Ecological Safety of Coastal and Shelf Zones of Sea*, (3), pp. 16–35.

Разномасштабная вихревая динамика на акватории Тихого океана, прилегающей к полуострову Камчатка и северным Курильским островам

А. В. Зимин [1] *, **Д. А. Романенков** [1], **А. А. Коник** [1], **О. А. Атаджанова** [1, 2], **Е. И. Свергун** [1], **А. В. Варкентин** [1, 3], **О. Б. Тепнин** [1, 3]

[1] *Институт океанологии им. П.П. Ширшова РАН, Москва, Россия*

[2] *Морской гидрофизический институт РАН, Севастополь, Россия*

[3] *Камчатский филиал ФГНБУ «ВНИРО», Петропавловск-Камчатский, Россия*

* *e-mail: zimin2@mail.ru*

Аннотация

Акватория шельфа и материкового склона Камчатского полуострова и северных Курильских островов со стороны Тихого океана является областью нереста и обитания некоторых видов промысловых рыб на ранних стадиях развития. Однако она остается недостаточно изученным районом океана с ограниченным набором данных наблюдений. Выполнен комплексный анализ разнородных спутниковых наблюдений и результатов расчетов по глобальной приливной модели за март – август 2015–2021 гг. Цель работы – получение новых сведений о пространственно-временной изменчивости характеристик разномасштабных вихревых структур и оценка влияния приливной динамики на некоторые особенности этой изменчивости. Используются следующие открытые архивы данных и атласы: *Mesoscale Eddy Trajectory Atlas Product Meta*3.2 *DT*, *MODIS-Terra*/*Aqua* и *VIIRS-Suomi NPP* (температура поверхности океана, концентрация хлорофилла *a*), радиолокационные изображения *Sentinel*-1*A*/*B*, ветер *NASA SMAP*, абсолютная динамическая топография *AVISO*, приливные течения *TPXO*9, течения *CMEMS GLORYS*12*v*1. По результатам анализа оценены межгодовая и сезонная изменчивость частоты встречаемости и характеристик мезомасштабных и субмезомасштабных вихрей и ее связь с вариациями Восточно-Камчатского течения и ветрового режима. Показан вклад прилива в вихревую динамику. В качестве примера рассмотрен случай проявления малых вихрей на периферии мезомасштабного антициклонического вихря в Авачинском заливе. Установлено, что взаимодействие антициклонической структуры с приливными течениями может служить самостоятельным механизмом генерации субмезомасштабных вихрей. Этот вывод может быть распространен для всего региона исследования, что представляется важным в понимании факторов, влияющих на выживание промысловых рыб на ранних стадиях развития.

Ключевые слова: вихрь, альтиметрия, спутниковая радиолокация, оптический диапазон, мезомасштабные вихри, субмезомасштабные вихри, прилив, течения, завихренность, минтай, Тихий океан

Благодарности: исследование выполнено за счет гранта Российского научного фонда № 23-17-00174, https://rscf.ru/project/23-17-00174/.

Для цитирования: Разномасштабная вихревая динамика на акватории Тихого океана, прилегающей к полуострову Камчатка и северным Курильским островам / А. В. Зимин [и др.] // Экологическая безопасность прибрежной и шельфовой зон моря. 2024. № 3. С. 16–35. EDN VPBEOU.

Introduction

The shelf and continental slope area of the Kamchatka Peninsula and the Northern Kuril Islands on the Pacific Ocean side represents an area of mass spawning and habitation of pollock (*Gadus chalcogrammus* Pallas) of the East Kamchatka population in the early stages of development. The pollock spawning in the region under consideration begins in March and ends in June [1]. Two types of spawning are identified: deepwater and shelf [2–4]. The first type is characteristic of areas with depths of 500–600 m, occurring in the tops of deepwater submarine canyons that extend into the shelves of Avacha and Kronotsky Gulfs. The second type is observed in areas with depths of 50–170 m and is mainly characteristic of the southeastern tip of Kamchatka and the Northern Kuril Islands [1]. Juvenile fish aggregations are concentrated in spawning areas and are abundant in the southern parts of the gulfs and shallow waters of the southeastern coast of Kamchatka [5]. Following hatching, the larvae ascend to the subsurface [2], where they must undergo development in the shelf zone in order to survive throughout the life cycle, from larvae to juveniles to fingerlings [6, 7]. Consequently, the study of distinctive characteristics of local water dynamics represents a priority task in elucidating the mechanisms influencing the yield of generations of East Kamchatka pollock.

The cold East Kamchatka Current and the associated eddy structures exert a considerable influence on the variability of the hydrological structure of the waters of the region under consideration [8, 9]. On average, the prevailing direction of water transport in the near-surface layer of the shelf and the continental slope of the peninsula is southwesterly. During the pollock spawning season, the current velocity varies from 5 to 45 cm/s [10]. At the same time, mesoscale eddies move relatively fast (with a velocity of ~ 4–5 cm/s), predominantly moving in the same direction [11]. Mesoscale structures of predominantly anticyclonic type, with a diameter of 70–150 km, are clearly discernible in the infrared and visible ranges and according to satellite altimeter data [12, 13]. The formation of these structures is attributed to the instability of the main current flow, with the generation areas influenced by the specific characteristics of the bottom topography and coastline, including the presence of extensive bays and capes along the oceanic coastline of the peninsula. Notable bays include Avacha Gulf, which is a primary pollock spawning ground [3], and is predominantly characterised by background anticyclonic circulation [14, 15] due to the influence of bottom relief and shoreline heterogeneities. Mesoscale eddies, determined from a variety of data sources, are often observed in the gulf, affecting the variability of water mass characteristics and the mixing of biologically productive coastal and oceanic waters [10, 16]. In particular, such formations may provide nutrients to the subsurface ocean and determine the level of phytoplankton development.

Note that at the periphery of mesoscale structures, according to satellite radar observations in the bays of the Kamchatka Peninsula, groups of eddy structures with sizes predominantly up to 5 km are recorded [17, 18]. Eddies of such sizes are classified as submesoscale, with the upper boundary of this category determined by the characteristic value of the internal Rossby radius. In the Pacific Ocean waters adjacent to the Kamchatka Peninsula and the Northern Kurils, the value of the baroclinic Rossby radius has been observed to vary from 4 to 15 km [19]. However, no systematic generalisation of data on the frequency of occurrence of small (submesoscale) eddies and the peculiarities of their generation has been made for this region. Submesoscale eddies are widespread in the World Ocean as a whole [20] and can play a significant role in the intensification of mixing, horizontal and vertical transport of heat and matter in local water areas [21]. The mechanisms responsible for the generation of small eddies are quite diverse [22] and include baroclinic-barotropic instability in the region of currents and frontal zones; topographic effects during the flow around seamounts, islands, and peninsulas; spatially inhomogeneous wind effects; interaction of larger eddies and their dissipation; water exchange through straits; and tidal dynamics. The role of these processes in the development of submesoscale water dynamics in the study area has yet to be evaluated. However, the importance of tidal processes, particularly those occurring in a spring-neap cycle, has been highlighted by [23] for the Northern Kuril Islands. It can be assumed that the intensive tidal dynamics observed in the water area under consideration, as evidenced in the Arctic seas [21, 24], can be a key factor on scales ranging from hundreds of metres to tens of kilometres and time intervals spanning minutes to days, corresponding to the submesoscale interval of hydrological field variability. Accordingly, the role of tides in shaping the features of submesoscale dynamics, which may have a significant impact on pollock survival at early developmental stages in the gulfs of the Kamchatka Peninsula and the adjacent waters of the Northern Kuril Islands, remains an open question. This motivates the present study.

The objective of this study is to obtain new data on the spatial and temporal variability of the characteristics of multiscale eddy structures and to assess the influence of tidal dynamics on some of its features in the Pacific Ocean waters adjacent to the Kamchatka Peninsula and the Northern Kurils from March to August (during the spawning period and early stages of pollock development). This will be achieved by generalising multi-year satellite data archives with the use of model calculations of tidal currents.

Materials and methods

The analysis of mesoscale eddies in the region adjacent to the Kamchatka Peninsula and the Northern Kurils (Fig. 1) for the period from March to August 2015–2021 was based on daily information on the rotation type, centre position, and radius of each eddy. The data were obtained from the Mesoscale Eddy Trajectory Atlas Product Meta3.2 DT archive [1)], which is based on daily mean absolute

[1)] Available at: https://doi.org/10.24400/527896/a01-2022.005.YYMMDD [Accessed: 25 August 2024]

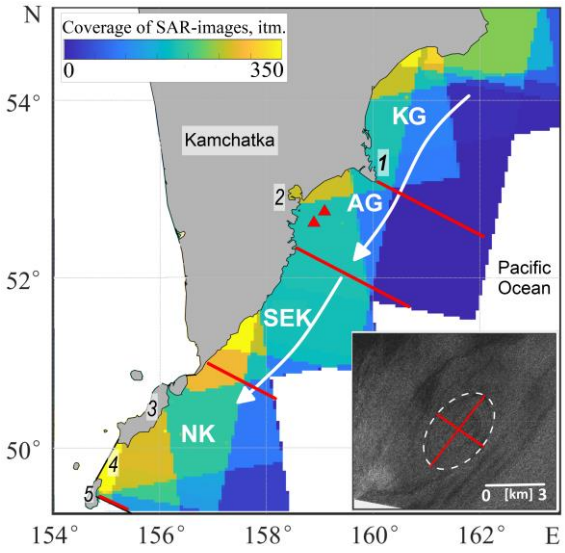

Fig. 1. Coverage of SAR images between March and August for 2015–2021: KG – Kronotsky Gulf; AG – Avacha Gulf; SEK – south-eastern Kamchatka; NK – northern Kuril Islands. *1* – Cape Shipunsky, *2* – Avacha Bay, *3* – Paramushir Island, *4* – Fourth Kuril Strait, *5* – Onekotan Island. The triangles indicate the Northern and Southern deepwater canyons in the Avacha Gulf. The white arrows show the main flow of the East Kamchatka Current. The inset shows an example of the manifestation of a cyclonic eddy structure on a SAR-image on 16 July 2016 at 19:57 UTC+0. The dashed line denotes the eddy boundary, the red lines are its large and small diameters

dynamic topography fields of the AVISO product with a spatial resolution of 0.25° × 0.25° in latitude and longitude.

Furthermore, instantaneous satellite fields of ocean surface temperature (OST) and chlorophyll a concentration from MODIS-Aqua, MODIS-Terra, VIIRS-Suomi NPP of L2 processing level with ~1 km resolution were additionally used (URL: https://oceancolor.gsfc.nasa.gov). A total of 3,160 fields were used for the days when mesoscale eddy manifestations were documented. The data that had quality indices of 0 (excellent) and 1 (good) based on the Near-infrared (NIR) algorithm evaluation [25] were selected. The fields were interpolated onto a grid corresponding to the fields of the absolute dynamic topography of the AVISO product. Subsequently, the temperature and chlorophyll a concentration at the centre and outer boundary of the mesoscale eddy, along with the horizontal gradient between them, were estimated.

A multi-year archive of Sentinel-1A/B high-resolution radar images (SAR) in C-band and Interferometric Wide (IW) imaging modes with a resolution of 20 m and a swath width of 250 km was used as initial data for recording surface manifestations of submesoscale eddies (URL: https://search.asf.alaska.edu/).

A total of 1,405 images covering the study region for the period from March to August 2015–2021 were analysed. The SAR coverage map of the region is presented in Fig. 1. Extreme irregularity in coverage can be evident, but in each of the selected areas, coverage varies from 50–100 SAR images over deepwater areas to 300–350 SAR images in coastal areas. The mean number of images per area is approximately 170.

As surface manifestations of submesoscale eddies, structures formed by thin dark or, conversely, bright light bands twisted into spirals or arcs were recorded on the SAR images (Fig. 1 inset). The structures observed in the images were predominantly the result of the film mechanism, while eddies caused by ice and shear waves were noted on fewer occasions [26]. As in previous studies [24, 27], eddies were detected visually from the manifestations described above, and their characteristics were determined based on the characteristics of the inscribed ellipse. The following characteristics we ere identified: centre coordinates, diameter (calculated as the mean between the large and small diameters) and type of rotation. The counterclockwise spiral was taken as a manifestation of the eddy with the cyclonic type of rotation and the clockwise spiral – with the anticyclonic type of rotation.

The analysis employed monthly average NASA SMAP [2)] (Soil Moisture Active Passive) scatterometer data with a spatial resolution of 0.25° in latitude and longitude for the period March to August 2015–2021. These data were used to examine the characteristics of the drive wind.

Surface currents were estimated using monthly mean zonal and meridional component data from the GLOBAL OCEAN PHYSICS REANALYSIS product [3)] (CMEMS GLORYS12v1) for 0–10 m horizons for March–August 2015–2021. Additionally, geostrophic currents from the AVISO altimetry product were used (URL: https://doi.org/10.48670/moi-00148). The background relative vorticity was calculated according to the method described in [28].

The characteristics of tidal currents were estimated from TPXO9 atlas data [29] at a resolution of 1/30° in latitude and longitude. Using TMD software (URL: https://github.com/EarthAndSpaceResearch/TMD_Matlab_Toolbox_v2.5) for selected points in the four sub-areas shown in Fig. 1, the total tide was precalculated for the eight main harmonic components ($M2$, $S2$, $N2$, $K2$, $K1$, $O1$, $P1$, $Q1$) for the entire study period. Secondary (nonlinear and long-period) harmonics were not taken into account, since special attention was paid to the variability of the characteristics of currents within a spring-quadrature cycle equal to half a lunar month. In order to obtain the results of the tidal current calculations for each of the four sub-areas shown in Figure 1, the data was taken from a single point, which was located above the sub-area signature. The tidal current field for the Avacha Gulf on 26.06.2018 was calculated using a 1/30° grid.

[2)] Available at: https://podaac.jpl.nasa.gov [Accessed: 25 August 2024].

[3)] Available at: https://doi.org/10.48670/moi-00021

Results

Mesoscale eddies. In the Pacific Ocean water area adjacent to the Kamchatka Peninsula and the Northern Kurils, 351 manifestations of mesoscale eddies with an average diameter of 90 km were recorded from March to August 2015–2021. Among the structures, the predominance of anticyclonic eddies (211) over cyclonic eddies (140) was noted, with the diameters of cyclones being on average larger than those of anticyclones.

Figure 2, *a* illustrates the spatial distribution of the trajectories of motion of mesoscale eddies over the specified period. The majority of eddies exhibiting both types of rotation (117 in total) were observed in the vicinity of the Kronotsky Gulf, whereas the greatest number of anticyclonic eddies (60 in total) were noted in the Avacha Gulf. The trajectories are presented in Fig. 2, *b*. It should be noted that only the characteristics of eddies falling within the areas of satisfactory coverage of the water area by SAR images were taken into account in the statistical analysis (see Fig. 1). However, due to the inherent limitations of altimetric measurements, the eddies in the immediate vicinity of the shoreline were not detected.

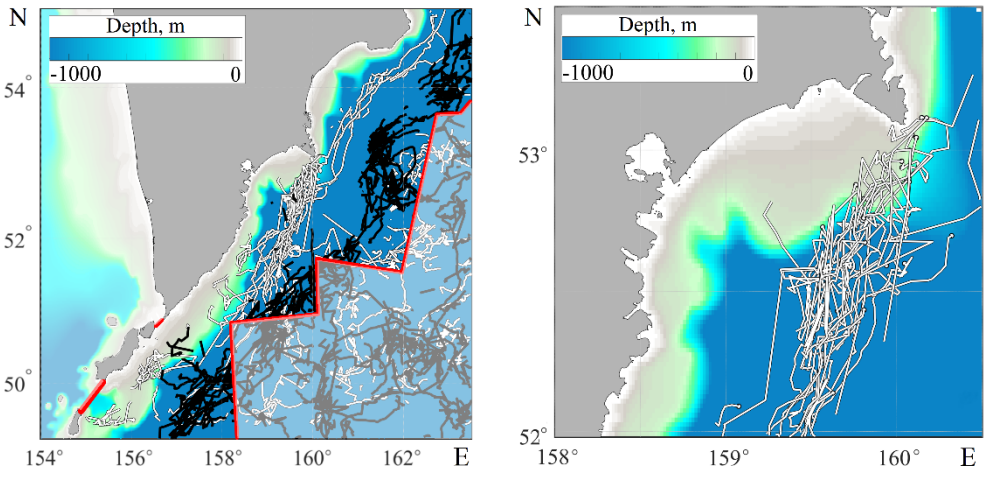

Fig. 2. Trajectories of mesoscale eddy movement in the areas adjacent to the Kamchatka Peninsula and the Kuril Islands from March to August 2015–2021 (*a*): the black lines indicate the cyclonic structure trajectories; the white lines indicate the anticyclonic structure trajectories. The red broken line limits the coastal area corresponding to the zone of satisfactory coverage of SAR images; tracks of anticyclonic mesoscale eddies near the Avacha Gulf (*b*)

In the study area, most of the mesoscale eddies move in a southwesterly direction, being formed as a result of the baroclinic instability [30] and interaction of the main flow of the East Kamchatka Current with bottom topography and large-scale irregularities of the coastline [9]. The known asymmetry in the distribution of cyclones and anticyclones relative to the current jet is confirmed [9]. Anticyclonic eddy structures tend to move closer to the coast and have an average lifetime of 21 days, while cyclonic structures tend to be more seaward and have a longer lifetime of 25 days. The main places of anticyclonic eddy formation are Kronotsky and Avacha gulfs, and less frequently these eddies occur in the shelf areas near the southern ends of capes jutting out into the sea, near Onekotan Island and the Fourth Kuril Strait. Intense eddy motion in these areas can influence the position and structure of cold and warm intermediate layers [31] and shape the distribution of abiotic environmental factors that determine the development of pollock eggs and larvae [3, 5].

On average, about 50 mesoscale eddy structures (Fig. 3, *a*) with a diameter of 90 km are observed in the study area from March to August each year. The interannual variability of their number does not exceed ±20 % and their mean diameter ±10 %. The year 2021 is anomalous in terms of the number of eddies. That year, the Kamchatka Current, especially in the spring months, deflected significantly to the southeast of the coast, forming a strong anticyclonic ring after passing Cape Shipunsky at the crossing of Avacha Gulf [10]. In 2016 and 2017, when the number of eddy structures was higher than the average, the East Kamchatka Current was pushed towards the coast and its velocity was above or close to the multi-year average.

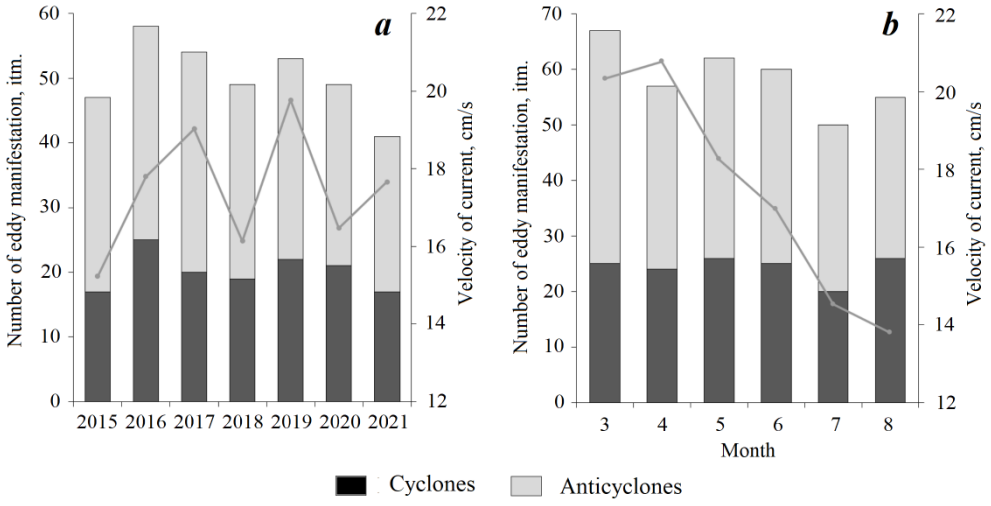

F i g . 3 . Distribution of the number of mesoscale eddies and average velocity of currents (gray line) in the upper layer based on CMEMS reanalysis data by years (*a*) and months (*b*)

Analysis of the intra-annual variability showed (Fig. 3, *b*) that the maximum number of eddy structures (65) was recorded in March and the minimum (50) in July. The observed maximum of manifestations is probably related to the weakening of the East Kamchatka Current due to rearrangement of atmospheric processes determined by the shift in the position of the Aleutian minimum [32, 33]. This is also confirmed by the seasonal change in surface current velocity from 21 cm/s in April to 14 cm/s in August, as observed in the CMEMS GLORYS12v1 reanalysis data. There are no significant seasonal trends in the variability of mean eddy diameters (diameters vary from 87 to 95 km for different months).

A generalisation of the OST data showed that the mean core temperature of mesoscale anticyclones was 5.8 °C and that of cyclonic anticyclones – 6.7 °C. This distribution is probably related to the peculiarities of the formation of mesoscale structures. Anticyclones, formed mainly in the bays of the Kamchatka Peninsula, trap and retain cold and dispersed shelf waters [11, 34]. Cyclones formed at the eastern edge of boundary currents, to which the East Kamchatka Current belongs, trap and transport warm and saline water [35]. The calculated mean annual temperature gradient between the centre and the periphery was 1.2 °C per 0.25° for anticyclones and 0.7 °C per 0.25° for cyclones. The maximum surface temperature gradient associated with eddies reaches 5 °C per 0.25°. These gradient values are quite significant and similar to estimates for frontal zones of climatic origin [36]. In addition, the outer boundary of mesoscale anticyclonic eddies tends to exhibit significant

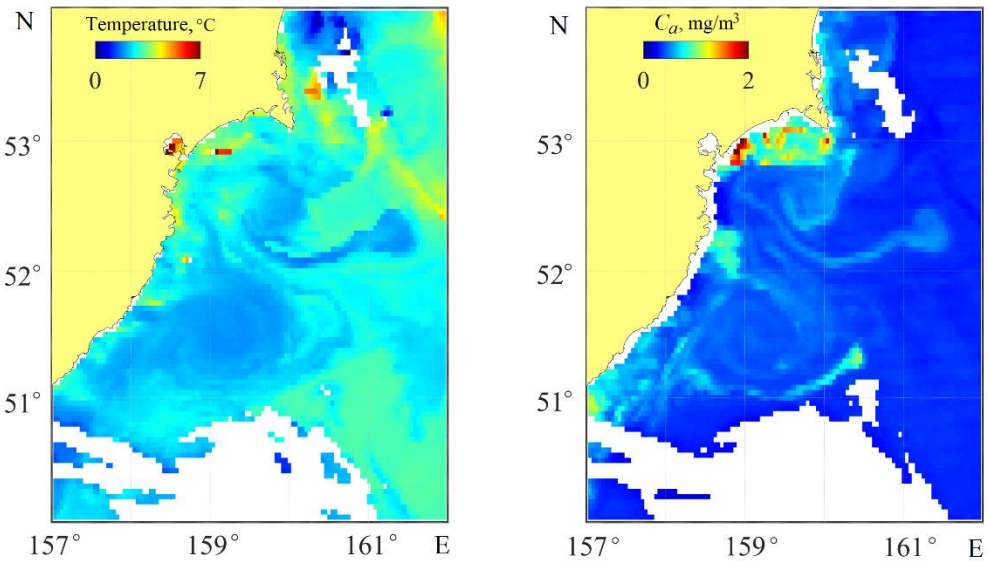

F i g . 4 . Manifestations of anticyclonic structures in fields of sea surface temperature (*a*) and chlorophyll a (*b*) according to MODIS spectroradiometer data from the Aqua satellite on April 26, 2017

gradients in chlorophyll a concentration (Fig. 4, *b*), averaging about 1.5 mg/m^3 per 0.25°, potentially making them areas of rich food resources favourable for pollock survival during early developmental stages [16].

Submesoscale eddies. In the study area during the warm period from 2015 to 2021, 559 surface manifestations of small (submesoscale) eddy structures were recorded, with diameters ranging from 300 m to 22.5 km, with a mean value of 3.4 km. In general, eddy structures are distributed over the whole area (Fig. 5, *a*), but they are mainly concentrated in the shelf zone and its coastal part. The most frequent manifestations are observed near the shores of the Kronotsky Gulf and near Avacha Bay (more than in every fifth to sixth SAR image), and also southeast of Paramushir Island (more than in every ninth to tenth SAR image). The dominance of eddies of the cyclonic type (428) over eddies of the anticyclonic type (131) can be seen. The mean diameter of eddies of both types was almost identical – 3.6 km for cyclones and 3.4 km for anticyclones.

Cyclonic eddy manifestations were most common at 2 to 4 km (Fig. 5, *b*) – about 40 % of all cyclones, and anticyclonic eddy manifestations – up to 2 km – about 30 % of all anticyclones. At the same time, almost 3/4 of all eddy manifestations had a diameter of up to 4 km, which corresponds to the minimum Rossby radius in the area [19]. In general, eddies of this diameter were found predominantly over the shelf or continental slope; large submesoscale eddies with a diameter of 10 km or more (about 5 %) were always found only over deep water.

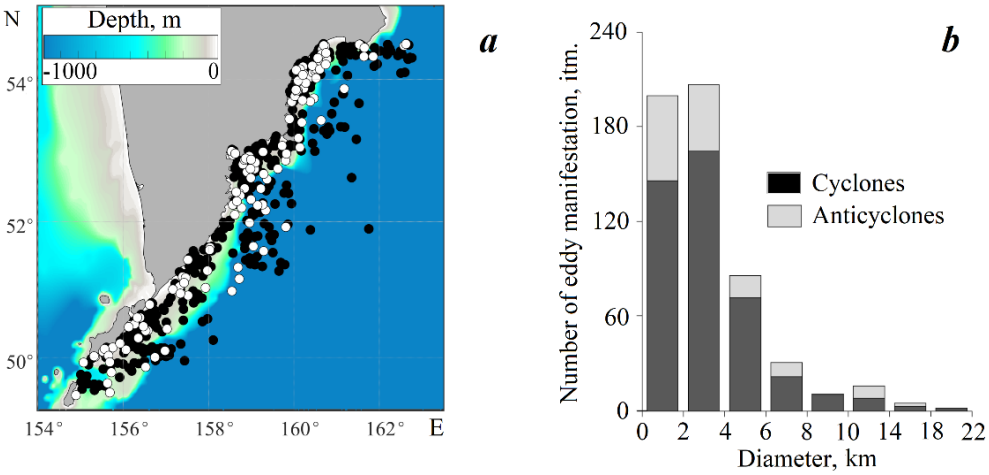

Fig. 5. Spatial distribution of centers of surface submesoscale eddy manifestations between March and August 2015–2021 (the black and white points indicate cyclonic and anticyclonic eddies, respectively) (*a*); the number of eddies depending on the diameter and type of rotation (*b*)

In 2015–2016, there were not many manifestations of submesoscale eddy structures (less than 10 % of the total number) due to low image availability in the area (Fig. 6, *a*). In 2017 and 2020, almost the same number of manifestations was recorded. As a rule, eddies were recorded on the shelf, most frequently in the Kronotsky Gulf in 2017, in the Avacha Gulf and near Paramushir Island in 2020. In 2018, eddies were most often observed in the form of groups. The maximum number of small eddies was observed in 2019 – 28 % of the total number. They were almost evenly distributed over the shelf, except for the area near Paramushir Island. In 2021, despite good data availability, few submesoscale eddies were detected. It is worth noting that the number of mesoscale eddy structures recorded this year is at an absolute minimum.

Regarding the description of the intra-annual variability of submesoscale activity, it should be noted that the monthly data availability for the period under consideration ranged from 221 to 240 SAR images. The minimum number of small eddies was recorded in March (Fig. 6, *b*). They were observed only as single eddies. In April, compared to March, the number of manifestations increased and they were more frequent in the shelf areas, especially in the Kronotsky Gulf. In May, the number of eddies increased, with the greatest increase recorded in the Avacha Gulf and near Paramushir Island. In June, almost 30 % of the total number of eddies were recorded. They were mainly recorded in groups. In July, the number of eddies decreased and they were mainly recorded in the Avacha Gulf.

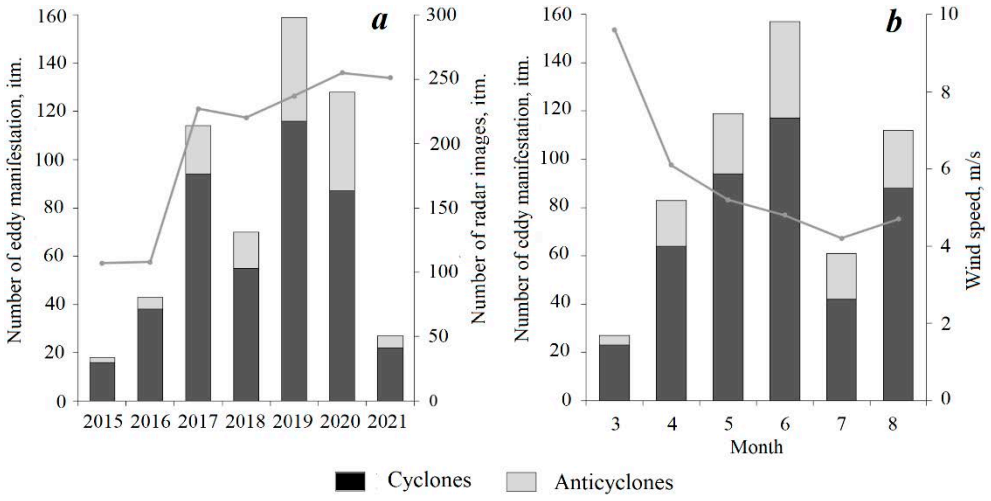

Fig. 6. Distribution of the number of registered manifestations of submesoscale eddies (bars) and the number of radar images (gray line) by year (*a*); intra-annual variability of the number of eddies (bars) and the average monthly speed of the surface wind (gray line) (*b*)

In August, the number of eddies increased again and they were observed more frequently over the shelf. Note that the minimum number of eddies in March can be explained by sufficiently high wind speeds (Fig. 6, *b*), which can lead to their masking on SAR images [37]. In other months, the average wind speed decreases to 5–6 m/s and does not prevent the manifestation of eddy structures on the SAR images, although another minimum in the number of submesoscale eddies is noted in July.

The obtained significant archive of one-time manifestations of submesoscale and mesoscale eddy structures allowed us to consider them together. A preliminary analysis of the coincident data showed that groups of small cyclonic eddies were often observed at the periphery of mesoscale anticyclones. The causes of eddy formation are quite diverse and typical for eddies of different scales [11, 26]. As noted in [26], small-scale eddy structures can be caused by local wind effects, shear instability of currents and frontal dynamics, plume propagation processes, and topographic effects when flowing around shoreline and bottom irregularities. The clustering of submesoscale eddies may indicate the transformation or even destruction of larger eddies. The role of tidal dynamics in this process is a poorly understood phenomenon.

Multiscale eddies and tidal dynamics. The cumulative analysis of satellite imagery showed that intense flow friction at the outer boundary of large eddies repeatedly formed a large number of submesoscale eddies. A total of 76 mesoscale eddies were identified based on the multi-year estimates obtained, with small eddies recorded at the outer boundary of these eddies. It is worth noting that in most cases such a situation occurred during the period of spring-like intensification of the tidal currents. The results of such analyses taking into account the tidal dynamics are presented in the table.

The table shows that the largest number of small eddies near mesoscale structures was observed in Avacha Gulf and the smallest – in the water area near the southeastern tip of Kamchatka. Up to 60 % of the small eddies are generated at the periphery of mesoscale structures during the spring tide. Typically, up to 10 small eddies per day were recorded at the periphery of mesoscale structures at maximum tidal current velocities.

Considering the fisheries interest in the Avacha Gulf area, we have considered here the case of synchronous registration of eddies of different scales, dated 26 June 2018. First, we note that during the period of March–August 2015–2021, 62 mesoscale anticyclones with diameters between 60 and 156 km crossed the Avacha Gulf (see Fig. 2, *b*). Most eddy structures are generated near Cape Shipunsky, move chaotically over the eastern part of the Avacha Gulf, and then dissipate south of 52° N with an average life of ~50 days. These eddies are often ‘delayed’ in the gulf, apparently falling into the area of weak velocities of the East Kamchatka Current. The eddies are clearly visible in the field of geostrophic velocities calculated from altimetric data (Fig. 7, *a*). Note also that the presence

Occurrence of small eddies in the areas adjacent to the Kamchatka Peninsula and the Kuril Islands from March to August 2015–2021

Area	Total number of SME	Including	
		at the ME periphery	of them during the spring tide
KG	189	80	40
AG	131	117	77
SEK	102	73	31
NK	137	94	65

Note: The occurrence was assessed if there were two or more eddies. SME – submesoscale eddies; ME – mesoscale eddies; KG – Kronotsky Gulf; AG – Avacha Gulf; SEK – south-eastern Kamchatka; NK – the northern Kuril Islands (see Fig. 1)

of the mesoscale eddy in Fig. 7, *a* is not confirmed by the CMEMS GLORYS12v1 reanalysis data. On the same day, 26.06.2018, radar data on the periphery of the mesoscale eddy, mainly in its northwestern part, revealed several submesoscale eddies with an average diameter of 1.5 km, indicated by the points in Fig. 7, *a*. As can be seen from Fig. 7, *b*, the observations fall within the period two days before the maximum spring tide.

To illustrate the role of tidal dynamics, we consider the variability of the total current vorticity in the tidal cycle. The eddy field corresponding to the geostrophic currents in the mesoscale eddy of Fig. 7, *a*, is shown in Fig. 7, *c*. Having chosen the closest moments of maximum tidal currents, we add them to the currents in the mesoscale eddy (assuming they are background) and then recalculate the eddy fields for these two moments. The difference between the two new vorticity fields is shown in Fig. 7, *d*, where it can be seen that the changes in total vorticity associated with the tidal influence are of the same order as its background values. It is clear that in the northwestern and northeastern parts of the mesoscale eddy there is a small-scale spatial inhomogeneity of the flow field when the tide is taken into account, which can be a source of submesoscale eddy generation. This is a manifestation of the known cascade process of vorticity transfer along the scale

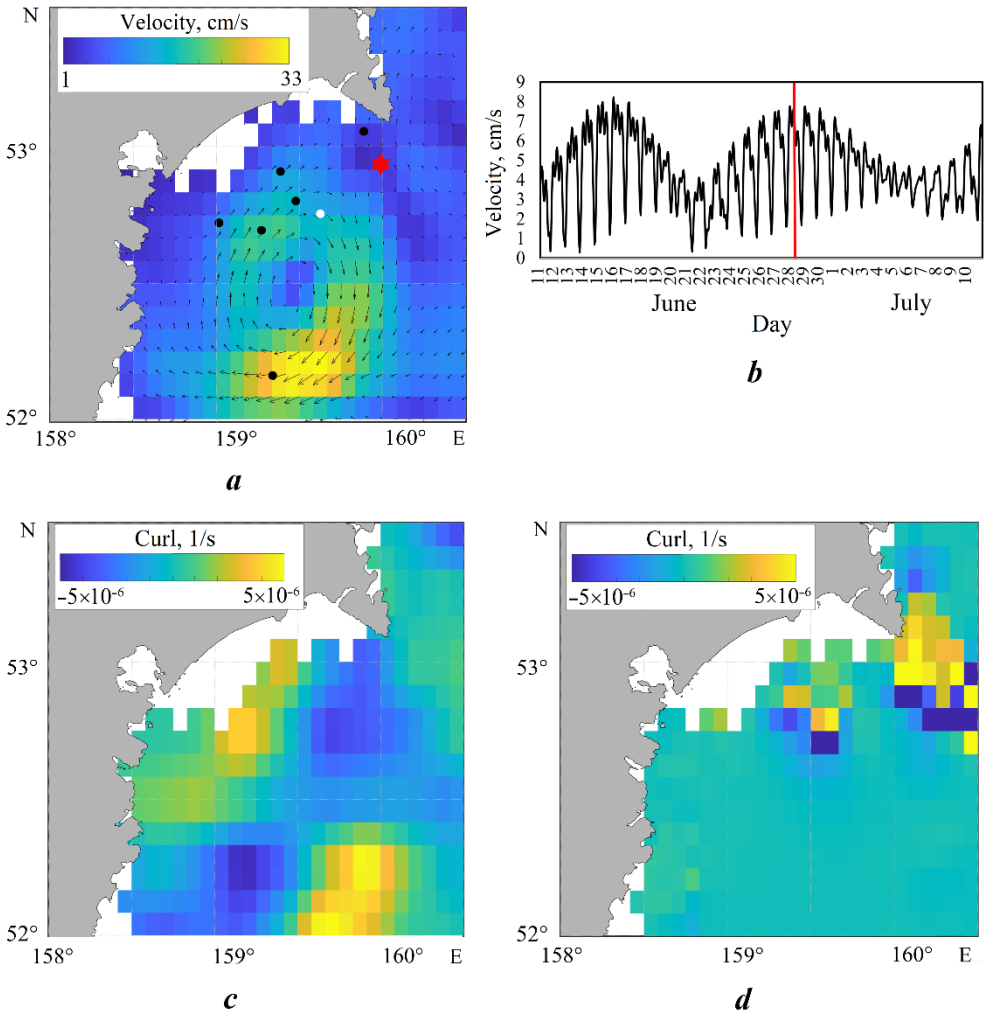

Fig. 7. Geostrophic circulation on 26.06.2018 with the position of the centers submesoscale eddy manifestations from Sentinel-1 SAR data (the red star is the point of tidal current calculation; the black and white points indicate cyclonic and anticyclonic submesoscale eddy structures, respectively) (*a*); the magnitude of tidal currents for 11.06–10.07.2018 (the red line indicates the time when small eddies were recorded on the SAR image) (*b*); the relative curl of the geostrophic circulation (*c*); the difference of the fields of total curl at high tide (04:00) and low tide (16:00) in the Avacha Gulf on 26.06.2018 (*d*). The geostrophic currents were interpolated onto the TPXO9 tidal model grid

spectrum from large to small scales [38]. The above considerations do not take into account the nonlinear interaction between the mesoscale eddy and the tide, baroclinic effects or other mechanisms of eddy formation are not considered. Nevertheless, the analysis presented together with the results of the table gives reason to consider the tidal factor in the occurrence of groups of small eddies as quite plausible, especially since almost all of these eddies are observed far from the coast at sufficiently large depths to exclude the influence of topographic effects. During the neap phase of the tidal oscillations, the currents are at least twice as weak here, and the tidal influence is reduced accordingly.

According to the OST data, the temperature of the core of the anticyclone during this period is 7.8 °C, while at the outer boundary the surface temperature reaches almost 9 °C. Thus, most of the small eddies are registered in the area of the high-gradient thermal zone. It is believed that submesoscale eddies contribute to more intensive vertical mixing and advection, which in turn may influence the surface distribution of chlorophyll a concentration in this part of the Avacha Gulf, which is favourable for biota development. Such a feature can be observed even in the spring period, similar to the one shown in Fig. 4. To conclude the analysis of the special case of 26.06.2018, we note another circumstance. The magnitude of tidal currents in the Avacha Gulf varies within a wide range. South of Cape Shipunsky they are comparable to the background currents and even exceed them. However, on dates close to the example under discussion, small eddies were not registered here due to the lack of radar coverage of this part of the Avacha Gulf.

Conclusion

This paper presents an analysis of heterogeneous satellite observations over the Pacific Ocean water area adjacent to the Kamchatka Peninsula and the Northern Kuril Islands. The comprehensive review of satellite data for a long period (seven years) in the region represents a novel contribution to the existing literature. The analysis demonstrated that eddy dynamics at different scales are subject to interannual and intra-annual variability in the frequency and locations of occurrence of eddy formations, as well as, to a lesser extent, in their size and type of rotation. The peculiarities of variability of mesoscale eddies are related to the behaviour of the East Kamchatka Current, which is largely determined by the atmospheric processes on the interannual and synoptic scales. As evidenced by satellite observations and literature sources, the variability in the characteristics of water masses and the dynamics of their boundaries observed in Avacha and Kronotsky Gulfs, as well as on the shelf of southeast Kamchatka, affects the life cycles of a variety of hydrobionts, including the early stages of pollock development.

The general trends in the interannual variability of submesoscale and mesoscale eddies are revealed. The intra-annual variability of the characteristics of multiscale eddies is demonstrated to depend on the peculiarities of seasonal fluctuations of the East Kamchatka Current and the wind regime.

The interconnection of eddies of varying scales provides an illustrative example of a theoretically described direct cascade of energy transfer in the ocean. The findings of our study indicate that the tidal factor can be a primary contributor to the formation of groups of smaller eddies at the periphery of larger mesoscale eddies, despite the absence of significant topographic effects. This phenomenon can be attributed to unsteady current velocity shifts that occur as a result of tidal currents. It can be hypothesised that such a process may result in the destruction of the mesoscale eddy, as well as influencing the vertical and horizontal distribution of pollock eggs and larvae. The specific example of the Avacha Gulf demonstrates the formation of small eddies in the area of mass spawning and larval development. The data on ocean surface temperature and chlorophyll concentration in the same area indicate that small eddies can exert a significant influence on the development of the prey base, which is of particular importance during the early stages of fish development. It would be highly beneficial to conduct *in situ* observations in order to describe these processes in greater detail.

It is noteworthy that the results of the global, widely used CMEMS ocean reanalysis GLORYS12v1 do not reflect the observed pattern of mesoscale eddies in the Avacha Gulf, which is indicative of multi-scale eddy dynamics in the region. This confirms the need to develop and improve high-resolution models for this region, which motivates further research.

REFERENCES

1. Buslov, A.V. and Tepnin, O.B., 2007. Characteristics of Walleye Pollock Spawn near the Northern Kurile Islands and the Southeast Extremety of Kamchatka. *The Researches of the Aquatic Biological Resources of Kamchatka and the North-West Part of the Pacific Ocean*, (9), pp. 235–245 (in Russian).
2. Buslov, A.V. and Tepnin, O.B., 2002. Conditions of spawning and embryogenesis of pollock Theragra chalcogramma (Gadidae) in deep-water canyons of the Pacific coast of Kamchatka. *Voprosy Ihtiologii*, 42(5), pp. 617–625 (in Russian).
3. Buslov, A.V., Tepnin, O.B. and Dubinina, A.Yu., 2004. Some Features of Spawn Ecology and Embriogenesis of the East Kamchatka Walleye Pollock. *Izvestiya TINRO*, 138, pp. 282–298 (in Russian).
4. Sergeeva, N.P., 2019. Spawning Intensity Walleye Pollock in Kronotsky Gulf (Eastern Kamchatka). In: A. M. Tokranov, ed., 2019. *Conservation of Biodiversity of Kamchatka and Coastal Waters : Materials of the XX International Scientific Conference, Dedicated to the 150th Anniversary of Academic V. L. Komarov's Birthday*. Petropavlovsk-Kamchatsky : Kamchatpress, 300 p. (in Russian).
5. Varkentin, A.I. and Saushkina, D.Y., 2022. Some Issues of Walleye Pollock Reproduction in the Pacific Waters Adjacent to the Kamchatka Peninsula and the Northern Kuril Islands in 2013–2022. *Trudy VNIRO*, 189, pp. 105–119. EDN HQAYWV. https://doi.org/10.36038/2307-3497-2022-189-105-119 (in Russian).
6. Shuntov, V.P., Volkov, A.F., Temnykh, O.S. and Dulepova, E.P., 1993. [*Walleye Pollock in Ecosystems of Far East Seas*]. Vladivostok: Izd-vo TINRO, 426 p. (in Russian).
7. Brodeur, R.D. and Matthew, T.W., 1996. A review of the Distribution, Ecology and Population Dynamics of age-0 Walleye Pollock in the Gulf of Alaska. *Fisheries Oceanography*, 5(S1), pp. 148–166. https://doi.org/10.1111/j.1365-2419.1996.tb00089.x
8. Terziev, F.S., ed., 1999. [*Hydrometeorology and Hydrochemistry of Seas. Vol. 10. The Bering Sea. Iss. 1. Hydrometeorological Conditions*]. Saint Petersburg: Gidrometeoizdat, 301 p. (in Russian).

9. Rogachev, K.A. and Shlyk, N.V., 2019. Characteristics of the Kamchatka Current Eddies. *Russian Meteorology and Hydrology*, 44(6), pp. 416–423. https://doi.org/10.3103/S1068373919060062

10. Tepnin, O.B., 2022. Variability of Hydrological Conditions at Spawning Sites of East Kamchatka Walleye Pollock (*Gadus chalcogrammus*) in 2012–2022. *The Researches of the Aquatic Biological Resources of Kamchatka and the North-West Part of the Pacific Ocean*, 66, pp. 79–93. https://doi.org/10.15853/2072-8212.2022.66.79-93 (in Russian).

11. Prants, S.V., 2021. Trench Eddies in the Northwest Pacific: An Overview. *Izvestiya, Atmospheric and Oceanic Physics*, 57(4), pp. 341–353. https://doi.org/10.1134/S0001433821040216

12. Vakulskaya, N.M., Dubina, V.A. and Plotnikov, V.V., 2019. Eddy Structure of the East Kamchatka Current According to Satellite Observations. In: POI FEB RAS, 2019. *Physics of Geospheres: The Collection of Scientific Articles on Selected Materials XI All-Russian Symposium "Physics of Geospheres"*. Vladivostok: V.I. Il'ichev Pacific Oceanological Institute. Iss. 1, 130 p. (in Russian).

13. Prants, S.V., Budynsky, M.V., Lobanov, V.B., Sergeev, A.F. and Uleysky, M.Yu., 2020. Observation and Lagrangian Analysis of Quasi-Stationary Kamchatka Trench Eddies. *Journal of Geophysical Research: Oceans*, 125(6), e2020JC016187. https://doi.org/10.1029/2020JC016187

14. Bondur, V., Zamshin, V., Chvertkova, O., Matrosova, E. and Khodaeva, V., 2021. Detection and Analysis of the Causes of Intensive Harmful Algal Bloom in Kamchatka Based on Satellite Data. *Journal of Marine Science and Engineering*, 9(10), 1092. https://doi.org/10.3390/jmse9101092

15. Alexanin, A., Kachur, V., Khramtsova, A. and Orlova, T., 2023. Methodology and Results of Satellite Monitoring of Karenia Microalgae Blooms, That Caused the Ecological Disaster off Kamchatka Peninsula. *Remote Sensing*, 15(5), 1197. https://doi.org/10.3390/rs15051197

16. Konik, A.A., Tepnin, O.B., Zimin, A.V., Varkentin, A.I., Atadzhanova, O.A., Sofina, E.V., Romanenkov, D.A., Svergun, E.I., Saushkina, D.Ya. and Rodikova, A.E., 2024. The Influence of Abiotic Factors on Alaska Pollock Distribution at the Early Stages of the Life Cycle in the Pacific Ocean Adjacent to the Kamchatka Peninsula. In: MSU, 2024. *Conference Proceedings of the XII International conference "Marine Research and Education" MARESEDU-2023. Moscow, 23–27 October 2023.* Tver: PoliPRESS. Vol. II(IV), pp. 308–318 (in Russian).

17. Kruglova, K.A., Zimin, A.V. and Atadzhanova, O.A., 2022. Comparative Analysis of the Characteristics of Surface Manifestations of Submesoscale Eddies in the Kuril-Kamchatka Region in the Summer 2020 and 2021. In: B. V. Chubarenko, ed., 2022. *Proceedings of the All-Russian Conference with International Participation "XXIX Coastal Conference: Field-Based and Theoretical Research in Shore Use Practice"*. Kaliningrad: Izdatelstvo IKBFU, pp. 460–463 (in Russian).

18. Zimin, A.V., Atadzhanova, O.A., Konik, A.A. and Kruglova, K.A., 2023. Small Eddy Structures of the Bering Sea and the Shelf of the Kuril-Kamchatka Region Based on Satellite Radar Data in the Warm Period 2020–2021. *Sovremennye Problemy Distantsionnogo Zondirovaniya Zemli iz Kosmosa*, 20(4), pp. 239–249 (in Russian).

19. Kurkin, A., Kurkina, O., Rybin, A. and Talipova, T., 2020. Comparative Analysis of the First Baroclinic Rossby Radius in the Baltic, Black, Okhotsk, and Mediterranean Seas. *Russian Journal of Earth Sciences*, 20(4), ES4008. https://doi.org/10.2205/2020ES000737

20. Thomas, L.N., Tandon, A. and Mahadevan, A., 2008. Submesoscale Processes and Dynamics. In: M. W. Hecht and H. Hasumi, eds., 2008. *Ocean Modeling in an Eddying Regime.* Washington : AGU, pp. 17–38. https://doi.org/10.1029/177GM04

21. Zimin, A.V., 2018. *Sub-Tidal Processes and Phenomena in the White Sea*. Moscow: GEOS, 220 p. (in Russian).

22. Payandeh, A.R., Washburn, L., Emery, B. and Ohlmann, J.C., 2023. The Occurrence, Variability, and Potential Drivers of Submesoscale Eddies in the Southern California Bight Based on a Decade of High-Frequency Radar Observations. *Journal of Geophysical Research: Oceans*, 128(10), e2023JC019914. https://doi.org/10.1029/2023JC019914

23. Nakamura, T., Matthews, J.P., Awaji, T. and Mitsudera, H., 2012. Submesoscale Eddies near the Kuril Straits: Asymmetric Generation of Clockwise and Counterclockwise Eddies by Barotropic Tidal Flow. *Journal of Geophysical Research: Oceans*, 117(C12), C12014. https://doi.org/10.1029/2011jc007754

24. Atadzhanova, O.A. and Zimin, A.V., 2019. Analysis of the Characteristics of the Submesoscale Eddy Manifestations in the Barents, the Kara and the White Seas Using Satellite Data. *Fundamental and Applied Hydrophysics*, 12(3), pp. 36–45. https://doi.org/10.7868/S2073667319030055

25. Goyens, C., Jamet, C. and Schroeder, T., 2013. Evaluation of Four Atmospheric Correction Algorithms for MODIS-Aqua Images over Contrasted Coastal Waters. *Remote Sensing of Environment*, 131, pp. 63–75. https://doi.org/10.1016/j.rse.2012.12.006

26. Karimova, S.S., 2012. Seasonal and Interannual Variability of Submesoscale Eddy Activity in the Baltic, Black and Caspian Seas. *Sovremennye Problemy Distantsionnogo Zondirovaniya Zemli iz Kosmosa*, 9(4), pp. 173–185 (in Russian).

27. Bashmachnikov, I.L., Kozlov, I.E., Petrenko, L.A., Glok, N.I. and Wekerle, C., 2020. Eddies in the North Greenland Sea and Fram Strait from Satellite Altimetry, SAR and High-Resolution Model Data. *Journal of Geophysical Research: Oceans*, 125(7), e2019JC015832. https://doi.org/10.1029/2019JC015832

28. Belonenko, T.V. and Sholeninova, P.V., 2016. On Identification of Mesoscale Eddies from Satellite Altimetry Based on the Area in the NW Pacific. *Sovremennye Problemy Distantsionnogo Zondirovaniya Zemli iz Kosmosa*, 13(5), pp. 79–90 (in Russian).

29. Egbert, G.D. and Erofeeva, S.Y., 2002. Efficient Inverse Modeling of Barotropic Ocean Tides. *Journal of Atmospheric and Oceanic Technology*, 19(2), pp. 183–204. https://doi.org/10.1175/1520-0426(2002)019<0183:EIMOBO>2.0.CO;2

30. Zhabin, I.A., Dmitrieva, E.V. and Taranova, S.N., 2021. Mesoscale Eddies in the Bering Sea from Satellite Altimetry Data. *Izvestiya, Atmospheric and Oceanic Physics*, 57(12), pp. 1627–1642. https://doi.org/10.1134/S0001433821120240

31. Zhabin, I.A., 2006. Evolution of the East Kamchatka Current Eddy as Detected by Satellite Observation. *Issledovanie Zemli iz Kosmosa*, (1), pp. 53–58 (in Russian).

32. Shlyk, N.V. and Rogachev, K.A., 2016. Rapid Freshening of the Kamchatka Current. *Vestnik of Far Eastern Branch of Russian Academy of Sciences*, (5), pp. 113–119 (in Russian).

33. Khen, G.V. and Zaochny, N.A., 2009. Variability of the Kamchatka Current Transport and Water Properties in the Kamchatka Strait. *Izvestija TINRO*, 158, pp. 247–260 (in Russian).

34. Bulatov, N.V. and Samko, E.V., 2002. [Main Features of the Frontal Zones Structure of the North-West Pacific Ocean]. *Izvestija TINRO*, 130-1, pp. 12–23 (in Russian).

35. Kubryakov, A.A., Belonenko, T.V. and Stanichny, S.V., 2016. Impact of Mesoscale Eddies on Sea Surface Temperature in the North Pacific Ocean. *Sovremennye Problemy Distantsionnogo Zondirovaniya Zemli iz Kosmosa*, 13(2), pp. 34–43 (in Russian).

36. Fedorov, K.N., 1986. *The Physical Nature and Structure of Oceanic Fronts*. New York: Springer-Verlag, 333 p.

37. Lavrova, O.Yu., Kostianoy, A.G., Lebedev, S.A., Mityagina, V.I., Ginzburg, A.I. and Sheremet, N.A., 2011. *Complex Satellite Monitoring of the Russian Seas*. Moscow: IKI RAS, 470 p. (in Russian).

38. Monin, A.S., Kamenkovich, V.M. and Kort, V.G., 1977. *Variability of the Ocean*. London: John Wiley & Sons Ltd., 241 p.

Submitted 13.05.2024; accepted after review 7.06.2024;
revised 17.06.2024; published 25.09.2024

About the authors:

Aleksey V. Zimin, Head of Laboratory, Shirshov Institute of Oceanology of Russian Academy of Sciences (30 1st Line of Vasilevsky Island, Saint Petersburg, 119053, Russian Federation), Dr.Sci. (Geogr.), **ResearcherID: C-5885-2014, Scopus Author ID: 55032301400**, *zimin2@mail.ru*

Dmitry A. Romanenkov, Leading Research Associate, Shirshov Institute of Oceanology of Russian Academy of Sciences (30 1st Line of Vasilevsky Island, Saint Petersburg, 119053, Russian Federation), Ph.D. (Geogr.), **ResearcherID: U-8280-2017, Scopus Author ID: 6506855768**, *dmromanenkov@yandex.ru*

Aleksandr A. Konik, Research Associate, Shirshov Institute of Oceanology of Russian Academy of Sciences (30 1st Line of Vasilevsky Island, Saint Petersburg, 119053, Russian Federation), Ph.D. (Geogr.), **ResearcherID: AAB-7195-2020, ORCID ID: 0000-0002-2089-158X, Scopus Author ID: 57203864647**, *konikrshu@gmail.com*

Oksana A. Atadzhanova, Senior Research Associate, Shirshov Institute of Oceanology of Russian Academy of Sciences (30 1st Line of Vasilevsky Island, Saint Petersburg, 119053, Russian Federation), Research Associate, Marine Hydrophysical Institute of Russian Academy of Sciences (2 Kapitanskaya St., Sevastopol, 299011, Russian Federation), Ph.D. (Geogr.), **ResearcherID: R-7835-2018, Scopus Author ID: 57188718743**, *oksanam07@list.ru*

Egor I. Svergun, Research Associate, Shirshov Institute of Oceanology of Russian Academy of Sciences (30 1st Line of Vasilevsky Island, Saint Petersburg, 119053, Russian Federation), Ph.D. (Geogr.), **ResearcherID: AAC-7289-2020, ORCID ID: 0000-0002-9228-5765, Scopus Author ID: 57195066881**, *egor-svergun@yandex.ru*

Aleksandr I. Varkentin, Leading Research Associate, Shirshov Institute of Oceanology of Russian Academy of Sciences (30 1st Line of Vasilevsky Island, Saint Petersburg, 119053, Russian Federation), Deputy Head of Kamchatka branch of Federal State Budget Scientific Institution "Russian Federal Research Institute of Fisheries and oceanography" ("KamchatNIRO") (18 Naberezhnaya St., Petropavlovsk-Kamchatskiy, 683000, Russian Federation), Ph.D. (Biol.), *a.varkentin@kamniro.vniro.ru*

Oleg B. Tepnin, Senior Research Associate, Shirshov Institute of Oceanology of Russian Academy of Sciences (30 1st Line of Vasilevsky Island, Saint Petersburg, 119053, Russian Federation), Head of Oceanography Sector of Kamchatka branch of Federal State Budget Scientific Institution "Russian Federal Research Institute of Fisheries and Oceanography" ("KamchatNIRO") (18 Naberezhnaya St., Petropavlovsk-Kamchatskiy, 683000, Russian Federation), **ORCID ID: 0000-0001-9596-4336, ResearcherID: KIL-1378-2024**, *tenpin@yandex.ru*

Contribution of the authors:

Aleksey V. Zimin – article concept, complex analysis and interpretation of the results, final version of the manuscript

Dmitry A. Romanenkov – analysis and interpretation of the data on section *Multiscale eddies*, significant alterations while revising the article text

Aleksandr A. Konik – analysis and interpretation of the data on sections *Mesoscale eddies* and *Multiscale eddies and tidal dynamics*, work on the article draft

Oksana A. Atadzhanova – analysis and interpretation of the data on section *Submesoscale eddies*, writing the article draft

Egor I. Svergun – work on the data of section *Multiscale eddies and tidal dynamics*, work on the article draft

Aleksandr I. Varkentin – complex interpretation of the results, work on the article draft

Oleg B. Tepnin – complex data analysis, work on the article draft

All the authors have read and approved the final manuscript.